Photonic-Crystal Surface-Emitting Lasers: Review and Introduction of Modulated-Photonic Crystals

Susumu Noda, *Fellow, IEEE*, Kyoko Kitamura, Tsuyoshi Okino, Daiki Yasuda, and Yoshinori Tanaka

(Invited Paper)

***Abstract*—Photonic-crystal surface-emitting lasers (PCSELs) have attracted much attention for their unrivaled capabilities, such as broad area, coherent resonance, tailored beam patterns, and beam steering. In this paper, we first review the progress of PCSELs, then introduce a novel concept of modulated photonic-crystal surface-emitting lasers (M-PCSELs) for realizing both lasing oscillation and on demand, beam diffraction for any two-dimensional direction in free space without the need for external elements. This unique concept paves the way toward the development of semiconductor lasers with completely controllable beams.**

***Index Terms*—Photonic crystals, Semiconductor lasers.**

I. Introduction

SEMICONDUCTOR lasers have contributed to modern society over a wide range of fields, particularly tele- and data-communications and optical storage. To date, much interest has been devoted toward expanding the utility of semiconductor lasers for these fields, such as by widening their range of accessible wavelengths and improving their modulation speed. On the other hand, with regard to high-power applications, semiconductor lasers have had difficulty simultaneously achieving high output powers and high beam qualities, so their development has lagged behind that of other lasers, such as CO_2 and fiber lasers. Moreover, as with many other lasers, semiconductor lasers have not been capable of on-chip beam pattern, polarization, and direction control; these functionalities required the addition of external elements which forfeits the advantage of compactness for which semiconductor lasers are renowned. Now, with the development of photonic-crystal surface-emitting lasers (PCSELs) [1]–[15], which are a new type of semiconductor laser, this paradigm is expected to change; PCSELs are attracting attention for not only their simultaneous achievement of high output power and high beam quality, but also their exhibition of functionalities that are not easily achievable with other types of lasers, such as polarization and beam-pattern control as well as on-chip beam-direction control, which eliminates the need for bulky external optics.

In 1999, we and another group independently and almost coincidentally proposed a concept for using a two-dimensional photonic-crystal as the laser cavity of a semiconductor laser [1], [16]. In the other group, Meier *et al.* reported lasing in a structure possessing a triangular lattice photonic crystal and an organic gain medium [16]. This laser, however, did not exhibit coherent, two-dimensional resonance, a pivotal property of photonic crystal laser cavities. The resonance reported in [16] was based on the X- (or M-) point of the triangular-lattice photonic crystal, where the light waves propagating forward and backward along three different directions couple one dimensionally into each other, but not two-dimensionally among different directions, within the cavity [2]. On the other hand, we proposed the use of the Γ-point of a triangular-lattice, semiconductor-based photonic crystal [1], whose light waves propagate along three different directions and couple both one- and two-dimensionally to create truly coherent two-dimensional resonance [1], [2]. In addition, due to the nature of the Γ-point, emission can be obtained from the surface of the photonic crystal; we named the laser a PCSEL to reflect this property. Since then, the basic operating principles of photonic-crystal lasers and a variety of new functionalities have been developed, including polarization and beam pattern control, blue-violet wavelength emission using wide-band-gap materials, one-dimensional beam steering, and watt-class high-power operation with a high beam quality [3]–[15]. Recently, an even newer type of PCSEL that possesses a modulated photonic crystal structure (hereafter, a "Modulated Photonic-Crystal," or M-PC) has been proposed and developed [17]–[19]; this new type of laser (hereafter, a "Modulated Photonic-Crystal Surface Emitting Laser," or M-PCSEL) enables the on-demand, two-dimensional control of beam diffraction while simultaneously preserving two-dimensional resonance.

In this manuscript, we first give a review of the progress in PCSELs and then describe the newly developed M-PCSELs. In Section II, we explain the lasing principle, beam pattern control, and watt-class, high-beam quality lasing oscillation of PCSELs. In Section III, we describe the concept and development of M-PCSELs. In Section IV, we show experimental results of

Manuscript received February 25, 2017; revised April 14, 2017; accepted April 16, 2017. Date of publication April 24, 2017; date of current version July 19, 2017. This work was supported in part by the ACCEL from JST, in part by the Grant-in-Aid for Scientific Research from JSPS, in part by the C-PhoST from MEXT, Japan, in part by the collaboration with ROHM Co., Ltd., and in part by the Hamamatsu Photonics K. K. *(Corresponding author: Susumu Noda.)*

S. Noda, T. Okino, D. Yasuda, and Y. Tanaka are with the Department of Electronic Science and Engineering, Kyoto University, Kyoto 615-8510, Japan (e-mail: snoda@kuee.kyoto-u.ac.jp; t_okino@qoe.kuee.kyoto-u.ac.jp; yasuda.daiki@qoe.kuee.kyoto-u.ac.jp; ytanaka@qoe.kuee.kyoto-u.ac.jp).

K. Kitamura is with the Institute for the Promotion of University Strategy, Global Excellence, Kyoto Institute of Technology, Kyoto 606-8585, Japan, and also with the Department of Electronic Science and Engineering, Kyoto University, Kyoto 615-8510, Japan (e-mail: kyoko@kit.ac.jp).

Digital Object Identifier 10.1109/JSTQE.2017.2696883

1077-260X © 2017 IEEE. Translations and content mining are permitted for academic research only. Personal use is also permitted, but republication/redistribution requires IEEE permission. See http://www.ieee.org/publications_standards/publications/rights/index.html for more information.

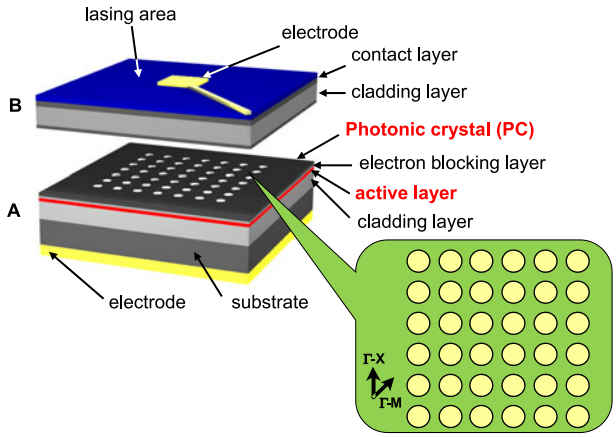

Fig. 1. Schematic image of a photonic-crystal surface-emitting laser (PCSEL). The photonic crystal is embedded near the active layer. The output beam is emitted from the surface of the device.

two-dimensional beam steering using these M-PCSELs, and we conclude with a summary in Section V.

II. Review of PCSELs: Lasing Principle, Beam-Pattern Control and Watt-Class, High-Beam Quality Lasing Oscillation

Early research on PCSELs, which focused on the basic laser principles, used triangular-lattice photonic crystals [1], [2]. This manuscript will focus on PCSELs with related, square-lattice photonic crystals (see Fig. 1), as it has since been found to be more suitable for high-power single-mode lasing oscillation as well as realizing various functionalities. For triangular-lattice photonic crystals, the reader is encouraged to refer to [2].

Fig. 2(a) shows the band structure of a square-lattice photonic crystal with a lattice constant of a; within this band structure exists a singularity point Γ (circled in red). At this point, four fundamental light waves propagating in the ±x and ±y directions couple between each other via higher-order Bloch waves. These waves are visualized in the reciprocal lattice space shown in Fig. 2(b), where the fundamental waves (gray arrows) have wave numbers $(\pm 2\pi/a, 0)$ and $(0, \pm 2\pi/a)$ and the higher-order Bloch waves (green arrows) have wave numbers that are larger integral multiples of $2\pi/a$. Here, coupling between the fundamental and higher-order waves are mediated by a variety of diffraction vectors $\boldsymbol{G}_{\mathrm{m,n}} = (\pm 2\mathrm{m}\pi/a, \pm 2\mathrm{n}\pi/a)$, where m and n are integers, that are generated by the periodicity of the photonic crystal. As a result, two-dimensional, broad-area cavity modes are generated at the band edges at the Γ-point; we label these band-edge modes A, B, C, and D as shown in Fig. 2(a). The four fundamental waves which form these band-edge modes can also be coupled to radiation modes outside the photonic crystal by the diffraction vectors $\boldsymbol{G}_{\pm 1,0} = (\pm 2\pi/a, 0)$ and $\boldsymbol{G}_{0,\pm 1} = (0, \pm 2\pi/a)$, which gives rise to the surface-emitted output beam. The efficiency of coupling to these radiation modes varies by band-edge mode. Modes C and D couple strongly to the radiation modes owing to their symmetric electric field distributions. Consequently, the threshold gain of each of these band-edge modes is so high that neither mode readily contributes to lasing. On the other hand, modes A and B couple only weakly to the radiation modes owing to their anti-symmetric (but rotationally symmetric) electric field distributions, so the lasing of either mode is possible. Stable single-mode lasing is achieved by further controlling the air-hole shape of the photonic crystal to create the final difference in threshold gain between modes A and B [3], [4], [15].

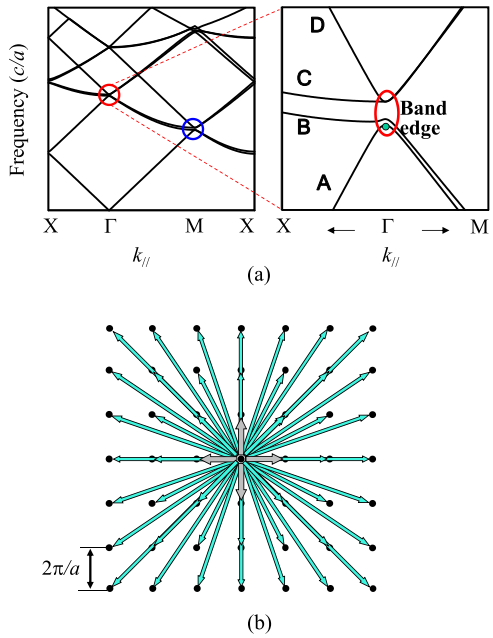

Fig. 2. (a) Band structure of a square lattice photonic crystal (left) and an enlarged image of this band structure around the Γ-band edges (right). The Γ-band edges are circled in red and the M-band edges are circled in blue. (b)Reciprocal lattice space of a square lattice photonic crystal. At the Γ-band edges, two-dimensional cavity modes are formed by the coupling of four fundamental wave vectors (gray arrows) mediated by a combination of high-order wave vectors (green arrows).

As seen in the structure of the PCSEL in Fig. 1, the photonic crystal layer is placed near the active layer so that gain can be provided to the band-edge modes via evanescent coupling. We initially developed a wafer-bonding technique [1], [13] to embed a photonic crystal structure inside the laser. The photonic crystal lattice constant a was chosen to overlap the gain curve of the active region to realize lasing at the band edge of the Γ-point. Fig. 3 shows the current-light output power characteristics and the near-field pattern and spectrum at various positions during lasing of this initial device. It is seen that room-temperature, continuous wave oscillation was successfully achieved, and the spectra was unchanged irrespective of its position of measurement. Note that the device was mounted right-side up, current was injected through a 50 μm × 50 μm area at the center of the photonic crystal, and the resonant light waves spread over a 150 μm × 150 μm area around the injection site. The lasing oscillation was found to occur at the band-edge mode A [4].

It has been also found that the beam pattern can be controlled with a variety of photonic crystal structures, each possessing unique air hole shapes and arrangements that were embedded inside the device (see Fig. 4). The current injection area of these devices (not shown) was 50 μm × 50 μm, and this entire

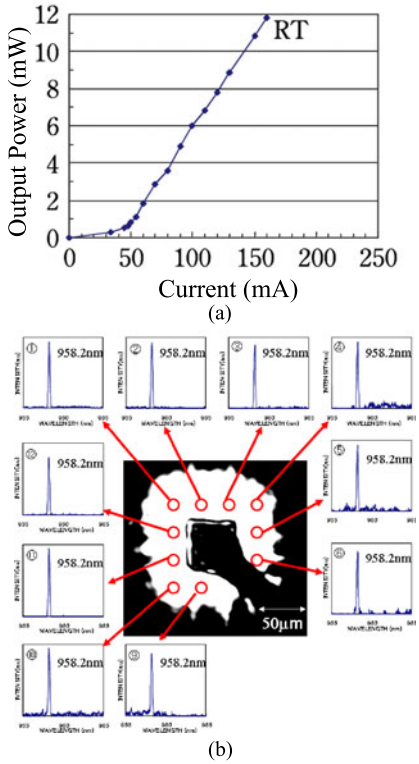

Fig. 3. Example of our initial PCSEL characteristics with room-temperature and continuous-wave operation: (a) light output power-current characteristics; (b) near-field pattern and spectra observed at various positions.

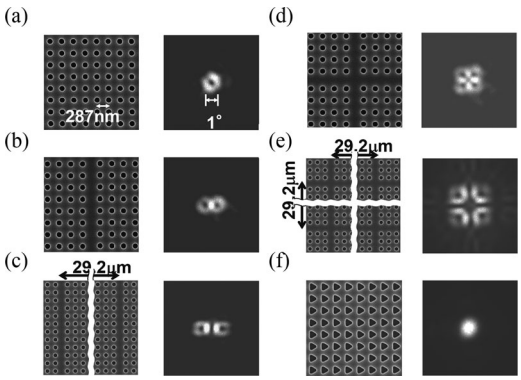

Fig. 4. Several beam patterns produced by PCSELs with engineered lattice points and/or lattice phases. Scanning electron microscope (SEM) images (left panels) and observed beam patterns (right panels) of photonic crystals with the following patterns are shown: (a) circular air holes with no lattice shift; (b) circular air holes with one shift; (c) circular air holes with parallel double shifts; (d) circular air holes with crossed shifts; (e) circular air holes with double-crossed shifts; and (f) triangular air holes with no lattice shift. A variety of output beam shapes including doughnuts and single lobes are obtained with these patterns.

area contained a single coherent mode. Corresponding to the arrangement of the photonic crystal, we obtained single-, twin-, and quadruple-doughnut shaped beams with circular air holes and also a single-lobed beam with triangular air holes [5]. The divergence angle of these beams was quite narrow (less than 1 degree) due to the effect of broad-area coherent resonance.

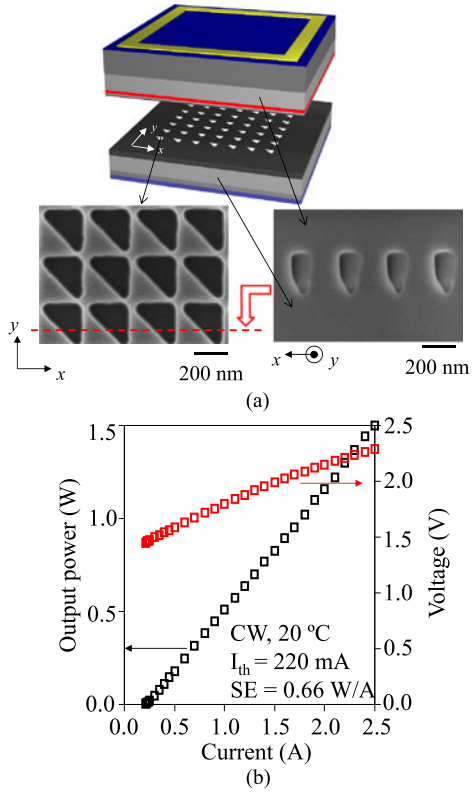

Fig. 5. Results of high-power-output, high-beam-quality operation of the PCSEL: (a) Schematic and SEM images of a PCSEL fabricated using the MOCVD regrowth method. The formation of material defects on the photonic crystal plane is suppressed. (b) Light output power-current characteristics (black dots) and voltage-current characteristics (red dots). Continuous-wave output powers of ∼1 W have been successfully realized.

We then investigated the ability of the PCSEL for high-power-output, high-beam-quality operation, for which we developed an advanced method of embedding the photonic crystal structure using a MOCVD regrowth technique in order to avoid the formation of material defects on the photonic crystal plane, which was previously observed in the wafer-bonding method. Upon optimizing the growth conditions, we have become able to fabricate devices while retaining the air holes within the photonic crystal layer as shown in Fig. 5(a). The device was mounted upside down, and the current was injected over an area of 200 μm $\times$ 200 μm. Continuous-wave output powers of ∼1 W have been successfully realized (see Fig. 5(b)) due to the significant suppression of defect formation on the photonic crystal plane. The oscillation was found to occur at the band-edge mode B of the Γ-point [15]. By virtue of the broad-area coherent resonance, the high-power, continuous-wave lasing of a single lateral and longitudinal mode was achieved, providing an exceptional beam quality M^2 of ∼1.09 [15]. This value is better than edge-emitting and vertical cavity surface emitting lasers, which do not control their lateral modes, at similar output powers. Further work, including the optimization of the photonic crystal structure and the widening of the active device area, will lead to the realization of much higher output powers (>10 W) while keeping M^2 very small. Such development will definitely contribute to

the development of next-generation, one-chip, ultra-compact, material-processing semiconductor lasers.

III. Principle and Development of M-PCSELs

Prospective applications such as laser radars, heads-up/mounted displays and automated driving require a laser whose beam direction can be controlled one-dimensionally, or even two-dimensionally, across a wide range of angles, yet is also compact, high-speed, and not dependent on any mechanical system. To address this requirement, we proposed in 2010 a new photonic crystal laser with a composite photonic-crystal structure composed of both square and rectangular lattices with varied relative lattice constants, and demonstrated that lasers based on this concept are able to emit beam to any direction in one dimension on demand [10].

In 2013, we discovered and developed an even more advanced type of laser called a M-PCSEL, which possesses the ability to emit a beam in not only one, but now two dimensions on demand. In this M-PCSEL, the air hole positions are shifted by a distance (d) and at an angle (ψ) from an original lattice position ($\boldsymbol{r}$) [17]–[19], where ψ (or d, or both) is modulated according to the diffraction which we want to introduce. For example, when we want to achieve a diffraction expressed by the vector $\boldsymbol{k}$, ψ is modulated according to the following equation:

$$\psi(\boldsymbol{r}) = \boldsymbol{k} \cdot \boldsymbol{r} \tag{1}$$

Then, the fundamental lightwaves which form the cavity mode are diffracted by the vector $\boldsymbol{k}$ to a region of reciprocal lattice space within the air light cone, from which they can couple to the radiation modes and be emitted to free space in a direction arbitrarily determined by $\boldsymbol{k}$. Note that because the air holes are modulated from their original positions in a periodic fashion, the M-PCSEL can also be called a "periodically-modulated photonic crystal laser" or a "position-modulated photonic crystal laser."

Now let us consider more concrete examples. Say we want to produce emission to some fixed direction by introducing a diffraction given by the vector $\boldsymbol{k}_0$. In this case, we modulate ψ according to (1) with $\boldsymbol{k} = \boldsymbol{k}_0$. If instead we want to introduce some distribution of diffractions given by a function of u around $\boldsymbol{k}_0$, the modulation ψ is given by (1) with the following $\boldsymbol{k}$ vector:

$$\boldsymbol{k} = \frac{\arctan\left[\iint A^{-1} u(\boldsymbol{k}' - \boldsymbol{k}_0)\exp(i\boldsymbol{k}' \cdot \boldsymbol{r}) d\boldsymbol{k}'\right]}{\boldsymbol{k}_0 \cdot \boldsymbol{r}} \boldsymbol{k}_0 \tag{2}$$

Equation (2) is derived using Fraunhofer diffraction theory; here, A^{-1} is a correction factor that can be used to correct the beam distribution following its observation. We note that the intensity of these diffractions can be controlled by d, which represents the magnitude of the shift of the individual air holes from their original positions.

To demonstrate the beam-steering ability of the M-PCSEL, we designed an M-PC structure with a constant diffraction vector $\boldsymbol{k} = \boldsymbol{k}_0$. Here, we must note that the diffraction vectors produce a surface-emitted beam in addition to and independent of that which is already emitted by the Γ-point band-edge modes as discussed in the previous section. To eliminate this inherent portion of the output beam, we use the M-point (circled in blue in Fig. 2(a)), which unlike the Γ-point lies outside the air light cone. At this M-point, the broad-area cavity mode is formed by four fundamental lightwaves with wavenumbers ($\pm\pi/a$, $\pm\pi/a$) (gray arrows in Fig. 6(a)) that couple to each other through the higher-order Bloch modes (green arrows in Fig. 6(a)) via a variety of diffraction vectors $\boldsymbol{G}_{\mathrm{m,n}} = (\pm 2\mathrm{m}\pi/a, \pm 2\mathrm{n}\pi/a)$. Then we introduce a $\boldsymbol{k}$ vector (solid red arrow in Fig. 6(b)) to diffract one of these fundamental lightwaves to a desired position inside the light cone in the reciprocal lattice space, which then couples to the radiation modes.

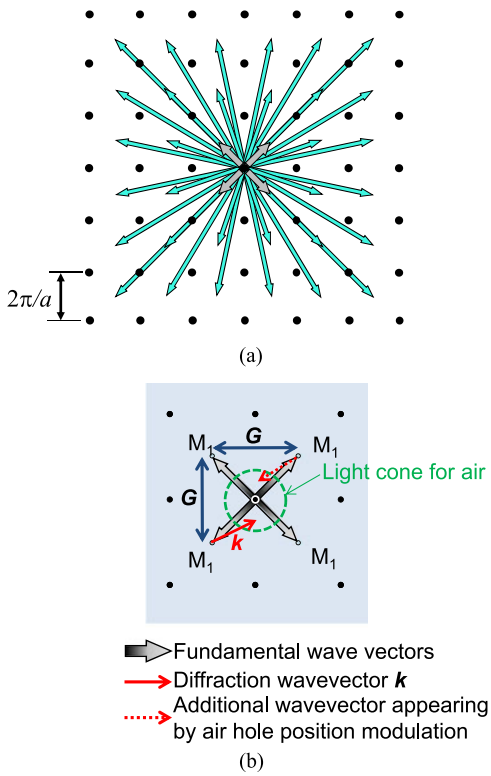

Fig. 6. (a) Reciprocal lattice space of a square-lattice photonic crystal. At the M-band edges, two-dimensional cavity modes are formed by the coupling of four fundamental wave vectors (gray arrows) mediated by a combination of high-order wave vectors (green arrows). (b) Coupling schematic in reciprocal lattice space. By introducing a k vector (red arrow), one of fundamental wavevectors (gray arrows) is diffracted to a desired position in the light cone, and then couple to the radiation modes and are emitted to free space. The dashed red line represents a $-k$ vector generated because the sign of the modulation ψ is indistinguishable in the finished photonic crystal structures.

In order to emit a beam into free space to a direction at angles of θ_{x} and θ_{y} from the surface normal of the photonic crystal in the x- and y-directions, respectively, $\boldsymbol{k}$ can be derived as:

$$\boldsymbol{k} = \left(\left(\frac{1}{2} - \frac{1}{\sqrt{2}n_{\mathrm{eff}}}\sin\theta_{\mathrm{x}}\right)\frac{2\pi}{a}, \left(\frac{1}{2} - \frac{1}{\sqrt{2}n_{\mathrm{eff}}}\sin\theta_{\mathrm{y}}\right)\frac{2\pi}{a}\right) \tag{3}$$

where the in-plane wavenumber conservation rule is considered, and n_{eff} is the effective refractive index of the device. Then, the

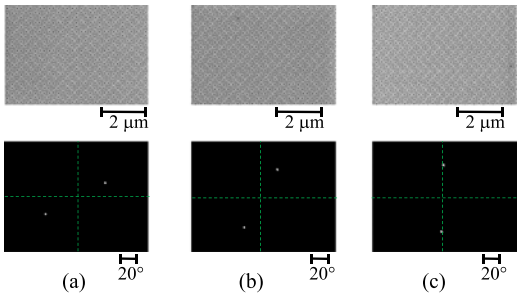

Fig. 7. Scanning electron microscope (SEM) images of M-PCs and their observed beam patterns. The M-PCs are designed with output beam angles of (a) $(\theta_x, \theta_y) = (33.8^\circ, 18.7^\circ)$, (b) $(\theta_x, \theta_y) = (18.7^\circ, 33.8^\circ)$, and (c) $(\theta_x, \theta_y) = (0.0^\circ, 40.0^\circ)$ with respect to the surface normal. All M-PCs have $a = 208$ nm and $d = 0.1a$.

following ψ is obtained:

$$\psi = \left(\frac{1}{2} - \frac{1}{\sqrt{2}n_{\text{eff}}}\sin\theta_x\right)\cdot\frac{2\pi}{a}\cdot x + \left(\frac{1}{2} - \frac{1}{\sqrt{2}n_{\text{eff}}}\sin\theta_y\right)\cdot\frac{2\pi}{a}\cdot y. \quad (4)$$

Fig. 7 shows scanning electron microscopy (SEM) images of M-PCs fabricated for emission to directions $(\theta_x, \theta_y) = (33.8^\circ, 18.7^\circ)$, $(18.7^\circ, 33.8^\circ)$, and (0.0°, 40.0°), where the deviation of the individual lattice points from their original positions is $d = 0.1a$. At a glance, the photonic crystals seem not to have any periodicity due to the modulation of the air-hole positions. The photonic crystals were fabricated to a size of 250 μm × 250 μm and embedded inside a device with electrode sizes of 50 μm × 50 μm. These devices successfully supported an oscillating, resonant mode, and they emitted light in the directions as designed (see Fig. 7(b)). Note that the emission occurred for both directions of $(\pm\theta_x, \pm\theta_y)$ because the sign of the modulation ψ is indistinguishable in the finished photonic crystal structures, and therefore the both $\pm\boldsymbol{k}$ vectors contributed to the diffraction of the fundamental waves (compare the solid and dashed red lines in Fig. 6(b)). The above results show that this seemingly randomized structure can indeed produce highly controllable, on-demand control of the beam direction.

IV. On-Chip Two-Dimensional Beam-Steering Enabled by M-PCSEL

We next engineered a structure that integrates the M-PC with various $\boldsymbol{k}$ vectors along the x- and y-planes in order to achieve gradual, continuous control of the output beam direction [20]–[22]. Here, we account for this continuous change by taking the space-derivative of both sides of (1):

$$\nabla\psi(\boldsymbol{r}) = \boldsymbol{k}(\boldsymbol{r}) \quad (5)$$

Using $\boldsymbol{k}$ given by (3), where θ_x and θ_y are assumed to be independent and linear functions of the x- and y-components of the photonic-crystal lattice point $\boldsymbol{r} = (x, y)$, respectively, ψ can be derived as follows:

$$\psi = \frac{2\pi}{a}\left(\frac{1}{2}x + \frac{1}{2}y - \frac{\cos\theta_x}{\theta'_x\sqrt{2}n_{\text{eff}}} - \frac{\cos\theta_y}{\theta'_y\sqrt{2}n_{\text{eff}}}\right) \quad (6)$$

where θ''_x and θ''_y are neglected following the assumption that θ_x and θ_y are linear functions.

To realize beam steering for θ_x from θ_{x1} to θ_{x2} and for θ_y from θ_{y1} to θ_{y2}, θ_x and θ_y can be expressed as

$$\theta_x = \theta_{x1} + \frac{\theta_{x2} - \theta_{x1}}{L_x}x \quad (7)$$

$$\theta_y = \theta_{y1} + \frac{\theta_{y2} - \theta_{y1}}{L_y}y \quad (8)$$

where L_x and L_y are the lengths of the photonic crystal in the x and y directions, respectively. Equations (6)–(8) are used to design and fabricate the actual M-PCSEL. As a test sample, we assigned $\theta_{x1} = 20^\circ$, $\theta_{x2} = 34^\circ$, $\theta_{y1} = 14^\circ$, $\theta_{y2} = 0^\circ$, $L_x = 303$ μm, and $L_y = 285\,\mu$m. After embedding the M-PC into the device, three kinds of electrodes, having areas and separations of, respectively, 15 μm × 15 μm and 3 μm, 33 μm × 15 μm and 3 μm, and 15 μm × 33 μm and 3 μm, were formed along the lateral and vertical directions in the shape of an L as shown in Fig. 8 (a). The individual electrodes were connected to an external driving circuit with integrated electrical wiring, as also shown in the figure. The sequence of electrodes along the horizontal and vertical arms of the L shape were arranged to steer the output beam in the x and y directions, respectively: From positions (1) and (2) along the vertical arm θ_y is designed to vary from 0° to 14° while keeping $\theta_x = 20^\circ$, and from positions (1) to (3) along the horizontal arm θ_x is designed to vary from 20° to 34° while keeping $\theta_y = 0^\circ$.

The experimental far-field patterns are shown on the left- and right-hand sides of Fig. 8(a). The left-hand side shows the far-field patterns obtained while sequentially driving the electrodes along the vertical arm from positions (1) to (2). Here, we clearly observed the change in output beams as designed: θ_y was varied from 0° to 14° while θ_x was fixed at 20°. Note that a second beam was also observed for θ_y from 0° to –14° with $\theta_x = -20^\circ$ due to the indistinguishable sign of modulation ψ for the finished photonic crystal structures as described before. Meanwhile, the right-hand side shows the far-field patterns obtained while sequentially driving the electrodes along the horizontal arm from positions (1) to (3). Again, we clearly observed the change in output beams as designed: θ_x was varied from 20° to 34° while θ_y was fixed at 0°, and a second beam was also observed for θ_x from –20° to –34° with $\theta_y = 0^\circ$. We have included a supplementary animated GIF file which contains the images taken when switching the different electrodes over a series 30 steps. This will be available at http://ieeexplore.ieee.org. Separately, we also confirmed that when the balance of injection current is smoothly adjusted among three of four adjacent electrodes labeled from A to D in Fig. 8(a), the beam direction changes continuously from $\theta_x = 29.5$ degree to 30.6 degree as shown in Fig. 8(b).

The foregoing discussion has focused on successful two-dimensional beam steering using electrodes arranged in the

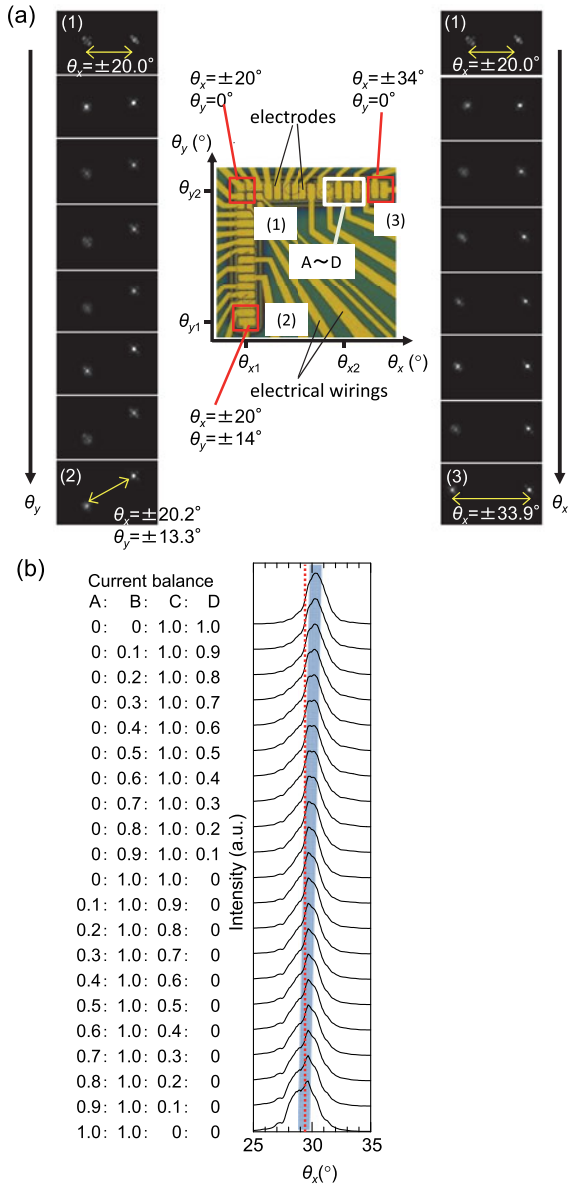

Fig. 8. (a) Far-field patterns and a captured image of multiple electrodes placed on the reverse side of the PCSEL. By switching electrodes from positions (1) to (2) vertically, the θ_y direction is changed; the experimental results of this process are shown on the left-hand side. Alternatively, by switching electrodes from positions (1) to (3) horizontally, the θ_x direction is changed; these results are shown on the right-hand side. (b) Change of far-field intensity profiles while tuning current from three adjacent electrodes (A-D; circled in white in Fig. 8(a)). The peak positions are finely tuned from $\theta_x = 29.5$ degrees to 30.6 degrees.

simple shape of an L, which covers a fraction of the total M-PCSEL area. Very recently, we have also succeeded in driving the full area of the M-PCSEL, which is important for achieving beam steering over a wider combination of angles. These latest results will be reported elsewhere.

V. Summary

We have reviewed the progress of PCSELs, including their lasing principle, beam-pattern control, and watt-class high-beam-quality lasing oscillation. Then, we have introduced the concept of M-PCSELs for uniting both lasing oscillation and beam control on-demand. We have shown that this unique concept enables two-dimensional beam steering without any external elements and paves the way toward the ultimate control of the output beam of semiconductor lasers. Such developments in PCSELs and M-PCSELs will contribute to the realization of next-generation, one-chip, ultra-compact lasers for various applications including material processing, laser radars, heads-up/mounted displays, and automated driving.

Acknowledgment

The authors would like to thank Dr. L. Yang, Dr. K. Ishizaki, Dr. T. Inoue, and Dr. T. Asano for fruitful discussions and helpful advice.

References

[1] M. Imada *et al.*, "Coherent two-dimensional lasing action in surface-emitting laser with triangular-lattice photonic crystal structure," *Appl. Phys. Lett.*, vol. 75, pp. 316–318, 1999.
[2] M. Imada, A. Chutinan, S. Noda, and M. Mochizuki, "Multidirectionally distributed feedback photonic crystal lasers," *Phys. Rev. B*, vol. 65, 2002, Art. no. 195306.
[3] S. Noda, M. Yokoyama, M. Imada, A. Chutinan, and M. Mochizuki, "Polarization mode control of two-dimensional photonic crystal laser by unit cell structure design," *Science*, vol. 293, pp. 1123–1125, 2001.
[4] K. Sakai *et al.*, "Lasing band-edge identification for a surface-emitting photonic-crystal laser," *IEEE J. Sel. Areas Commun.*, vol. 23, no. 7, pp. 1335–1340, Jul. 2005.
[5] E. Miyai *et al.*, "Lasers producing tailored beams," *Nature*, vol. 441, p. 946, 2003.
[6] S. Riechel *et al.*, "A nearly diffraction limited surface emitting conjugated polymer laser utilizing a two-dimensional photonic band structure," *Appl. Phys. Lett.*, vol. 77, pp. 2310–2312, 2000.
[7] H. Y. Ryu, S. H. Kwon, Y. J. Lee, and Y. H. Lee, "Very-low-threshold photonic band-edge lasers from free-standing triangular photonic crystal slabs," *Appl. Phys. Lett.*, vol. 80, pp. 3476–3478, 2002.
[8] M. Kim *et al.*, "Surface-emitting photonic-crystal distributed-feedback laser for the midinfrared," *Appl. Phys. Lett.*, vol. 88, 2006, Art. no. 191105.
[9] S. Iwahashi *et al.*, "High-order vector beams produced by photonic-crystal lasers," *Opt. Express*, vol. 19, pp. 11963–11968, 2011.
[10] K. Kitamura, M. Nishimoto, K. Sakai, and S. Noda, "Needle-like focus generation by radially polarized halo beams emitted by photonic-crystal ring-cavity laser," *Appl. Phys. Lett.*, vol. 101, 2012, Art. no. 221103.
[11] H. Matsubara *et al.*, "GaN photonic-crystal surface-emitting laser at blue-violet wavelengths," *Science*, vol. 319, pp. 445–447, 2008.
[12] Y. Kurosaka *et al.*, "On-chip beam-steering photonic-crystal lasers," *Nature Photon.*, vol. 4, pp. 447–450, 2010.
[13] D. Ohnishi, T. Okano, M. Imada, and S. Noda, "Room temperature continuous wave operation of a surface-emitting two-dimensional photonic crystal diode laser," *Opt. Express*, vol. 12, no. 8, pp. 1562–1568, 2004.
[14] T. Sakaguchi *et al.*, "Fabrication of photonic-crystal lasers by MOCVD regrowth technique(II)," presented at 71st Japanese Society Appl. Physics, Autumn Meeting, Nagasaki, Japan, Sep. 14–17, 2010, Paper 16p-J-10.
[15] K. Hirose *et al.*, "Watt-class high-power, high-beam-quality photonic-crystal lasers," *Nature Photon.*, vol. 8, pp. 406–411, 2014.
[16] M. Meier *et al.*, "Laser action from two-dimensional distributed feedback in photonic crystals," *Appl. Phys. Lett.*, vol. 74, pp. 7–9, 1999.
[17] S. Noda, T. Okino, K. Kitamura, Y. Tanaka, and Y. Liang, "Two-dimensional Photonic Crystal Surface-Emitting Lasers," Japanese Patent 6080941, Jan. 27, 2017.
[18] T. Okino, Y. Liang, K. Kitamura, and S. Noda, "Beam-direction control by modulated photonic-crystal lasers," presented at the 60th Japanese Society Applied Physics, Spring Meeting, Kanagawa, Japan, Mar. 27–30, 2013, Paper 28p-C1-17.
[19] T. Okino, K. Kitamura, D. Yasuda, Y. Liang, and S. Noda, "Position-modulated photonic-crystal lasers and control of beam direction and polarization", in *Proc. Conf. Lasers Electro, Opt.*, 2015, Paper SW1F.1.
[20] D. Yasuda, K. Kitamura, Y. Lee, and S. Noda, "Characteristic of modulated photonic-crystal laser for two-dimensional beam scanning," pre-

sented at 62nd Japanese Society Applied Physics, Spring Meeting, Kanagawa, Japan, Mar. 11–14, 2015, Paper 12p-A10-9.

[21] D. Yasuda, K. Kitamura, and S. Noda, "Investigation of photonic-crystal lattice and device structures of two-dimensional beam scanning photonic-crystal lasers (II)," presented at 76th Japanese Society Applied Physics, Autumn Meeting, Aichi, Japan, Sep. 13–16, 2015, Paper 16a-2A-13.

[22] D. Yasuda, A. Nishigo, K. Kitamura, and S. Noda, "Investigation of photonic-crystal lasers with two-dimensional beam scanning capability (III)," presented at 63rd Japanese Society of Applied Physics, Spring Meeting, Tokyo, Japan, Mar. 19–22, 2016, Paper 21a-S621-10.

Susumu Noda (M'92–SM'06–F'08) received the B.S., M.S., and Ph.D. degrees from Kyoto University, Kyoto, Japan, in 1982, 1984, and 1991, respectively, all in electronics, and the Honorary degree from Gent University, Gent, Belgium, in 2006. From 1984 to 1988, he was with the Mitsubishi Electric Corporation, and he joined Kyoto University in 1988. He is currently a full Professor in the Department of Electronic Science and Engineering and the Director of Photonics and Electronics Science and Engineering Center, Kyoto University. His research interest focuses on physics and applications of photonic nanostructures based on photonic crystals. He received various awards, including the IBM Science Award (2000), the Japan Society of Applied Physics Achievement Award on Quantum Electronics (2005), Optical Society of America Joseph Fraunhofer Award/Robert M. Burley Prize (2006), 1st the Japan Society of Applied Physics Fellow (2007), The Commendation for Science and Technology by the Minister of Education, Culture, Sports, Science and Technology (2009), the IEEE Nanotechnology Pioneer Award (2009), The Reo-Esaki Award (2009), Medal with Purple Ribbon (2014), and the Japan Society of Applied Physics Outstanding Achievement Award (2015).

Kyoko Kitamura received the B.S. and M.S. degrees in chemical engineering in 2006 and 2008, respectively, and the Ph.D. degree in electronics in 2011, from Kyoto University, Kyoto, Japan. From 2008 to 2011, she was a Research Fellow of the Japan Society for the Promotion of Science, Kyoto University. From 2011 to 2012, she was a Postdoctoral Fellow at Kyoto University. From 2012 to 2015, she was an Assistant Professor in the Hakubi Center for Advanced Reserch, Kyoto University. She is currently a Lecturer in the Institute for the Promotion of University Strategy, Global Excellence, Kyoto Institute of Technology, Kyoto, Japan. Her research interests include manipulation of laser beams using PCSELs and peculiar focusing properties and interaction with nano-structures in vector vortex beams. She received various awards, including Kyoto University the Tachibana Award for the Most Outstanding Female Researcher/the Students' Prize (2011), the Japan Society of Applied Physics Promotion and Nurturing of Female Researchers Contribution Award/the Young researchers' Prize (2015), and The Commendation for Science and Technology by the Minister of Education, Culture, Sports, Science and Technology/the Young Scientists' Prize (2016). She is a member of the Japan Society of Applied Physics and Optical Society of America.

Tsuyoshi Okino received the B.S. and M.S. degrees from Kyoto University, Kyoto, Japan, in 2012 and 2014, respectively, all in electronics. He is currently in Murata Manufacturing Co., Ltd, Nagaokakyo, Japan.

Daiki Yasuda received the B.S. and M.S. degrees from Kyoto University, Kyoto, Japan, in 2014 and 2016, respectively, all in electronics. He is currently in Asahi Kasei Microdevices Corporation, Tokyo, Japan.

Yoshinori Tanaka received the B.S., M.S., and Ph.D. degrees from Kyoto University, Kyoto, Japan, in 2001, 2003, and 2006, respectively, all in electronics. From 2003 to 2006, he was a Research Fellow in Japan Society for the Promotion of Science, Kyoto University. From 2006 to 2007, he was a Postdoctoral Fellow at Kyoto University, and from 2007 to 2015, he was an Assistant Professor in the Department of Electronic Science and Engineering, Kyoto University. He is currently a Junior Associate Professor in the GL center and the Department of Electronic Science and Engineering, Kyoto University, Kyoto, Japan. His current research interests include the theoretical analyzes of two-dimensional photonic crystals. He received the Young Scientist Presentation Award from Japan Society of Applied Physics (2005). He is a member of the Japan Society of Applied Physics.